Journal of Controlled Release 220 (2015) 79–88

Contents lists available at ScienceDirect

Journal of Controlled Release

journal homepage: www.elsevier.com/locate/jconrel

Heparin desulfation modulates VEGF release and angiogenesis in diabetic wounds

Uwe Freudenberg [a,1], Andrea Zieris [a,1], Karolina Chwalek [a], Mikhail V. Tsurkan [a], Manfred F. Maitz [a], Passant Atallah [a], Kandice R. Levental [a], Sabine A. Eming [b], Carsten Werner [a,*]

[a] Leibniz Institute of Polymer Research Dresden (IPF), Max Bergmann Center of Biomaterials Dresden (MBC), Technische Universität Dresden, Center for Regenerative Therapies Dresden (CRTD), Hohe Str. 6, 01069 Dresden, Germany

[b] Department of Dermatology, Center for Molecular Medicine Cologne (CMMC), Cologne Excellence Cluster on Cellular Stress Responses in Aging-Associated Diseases (CECAD), University of Cologne, Germany

ARTICLE INFO

Article history:
Received 10 July 2015
Received in revised form 28 September 2015
Accepted 14 October 2015
Available online 22 October 2015

Keywords:
Hydrogels
Glycosaminoglycans
Heparin
Growth factors
Angiogenesis
VEGF

ABSTRACT

While vascular endothelial growth factor (VEGF) has been shown to be one of the key players in wound healing by promoting angiogenesis current clinical applications of this growth factor to the wound environment are poorly controlled and not sustainable. Hydrogels made of sulfated glycosaminoglycans (GAG) allow for the sustained release of growth factors since GAGs engage in electrostatic complexation of biomolecules. In here, we explore a set of hydrogels formed of selectively desulfated heparin derivatives and star-shaped poly(ethylene glycol) with respect to VEGF binding and release and anticoagulant activity. As a proof of concept, supportive effects on migration and tube formation of human umbilical vein endothelial cells were studied *in vitro* and the promotion of wound healing was followed in genetically diabetic (db/db) mice. Our data demonstrate that the release of VEGF from the hydrogels is modulated in dependence on the GAG sulfation pattern. Hydrogels with low sulfate content (11% of initial heparin) were found to be superior in efficacy of VEGF administration, low anticoagulant activity and promotion of angiogenesis.

1. Introduction

Dermal wound healing is a dynamic process regulated by a multitude of growth factors and cytokines. Aging, obesity, diabetes, cardiovascular disorders and autoimmune diseases interfere with wound healing and can even cause non-healing, chronic wounds such as the diabetes foot ulcer [1]. Vascular endothelial growth factor (VEGF) has been shown to be one of the key players in wound healing by promoting angiogenesis [2–4]. Application of VEGF accelerated wound healing in diabetic rodents [5–9]. However, when administered topically, soluble growth factors rapidly delocalize in tissue fluids and become degraded by proteases in chronic wound environments [10,11]. Nevertheless, ulcer healing was found to be improved in clinical trials upon topical application of the VEGF gene-carrying plasmid (720 μg/m^2 every 48 h) to the foot ulcer surface [2,12]. A controlled-release system to protect and sustainably deliver VEGF during wound healing while avoiding overdosage may be highly beneficial in the advanced wound management [1,3].

In living tissues, cell surface heparan sulfate proteoglycans (HSPGs) are known to bind VEGF [2,3,13], resulting in stabilization and improved binding of VEGF to cell-surface receptors [5–7,14]. Heparin, an easily accessible highly sulfated glycosaminoglycan (GAG) produced in mast cells, exhibits sulfation patterns resembling those of heparan sulfate and binds a plethora of signaling molecules including VEGF [10,13]. Accordingly heparin-based matrices gained interest for growth factor delivery [2,12,15–23]. A modular starPEG-heparin hydrogel platform was recently introduced for the decoupling of physical network properties and biomolecular signaling characteristics [24–26]. The system is advantageous with respect to its mechanical properties (as required for wound dressings) and the high content of heparin allowing for an unperturbed loading and release of combinations of different factors (including VEGF), which was previously demonstrated to support morphogenesis of endothelial cells *in vitro* [26,27] and angiogenesis *in vivo* [27,28]. Adjusting the sulfation pattern of heparin by selective desulfation offers additional options for modulating uptake and release of VEGF [29] while avoiding hemorrhagic side effects. A set of selectively desulfated heparins was recently used in the formation of biohybrid hydrogels with starPEG and demonstrated to allow for decoupling mechanical and biomolecular characteristics as previously reported for the heparin-based gels [30]. Since the anticoagulant activity of heparin depends on a fully sulfated pentasaccharide sequence including the relatively rare 3-O sulfate [31,32], desulfation protocols covering this moiety were considered particularly suitable to avoid bleeding. In here, hydrogels with graded sulfation pattern, desulfated at 2-O, 6-O,

* Corresponding author.
E-mail address: carsten.werner@tu-dresden.de (C. Werner).
[1] Both contributed equally.

http://dx.doi.org/10.1016/j.jconrel.2015.10.028
0168-3659/

N-position, 6-O and N or 2-O, 6-O and N-position (complete sulfate removal) were synthesized and systematically studied with respect to VEGF-A (VEGF) binding and release as well as anticoagulant activity. Supportive effects of the modulated VEGF release on migration and tube formation of human umbilical vein endothelial cells (HUVECs) were examined *in vitro* and in the wound healing of diabetic (db/db) mice. The chosen set of experiments was intended to pave the way for potential future applications of the developed hydrogel system as VEGF releasing wound dressing (see Fig. 1).

2. Materials and methods

Unless otherwise indicated, all chemicals were purchased from Sigma-Aldrich, Munich, Germany. VEGF refers to recombinant VEGF-A (VEGF 165) from PeproTech, Hamburg, Germany.

2.1. Preparation of desulfated heparin derivatives

All desulfated heparin derivatives were prepared starting from the naturally occurring, fully sulfated heparin (SH; 14,000 g/mol; sodium salt, porcine intestinal mucosa, Calbiochem, Darmstadt, Germany).

2.1.1. Pyridinium heparinate [33–35]

35 g of Amberlite IR-120 H^+ ion exchange resin (Rohm and Haas, Philadelphia, USA) was filled in a glass column and washed with deionized water, regenerated for 30 min with 10% aqueous HCl, and washed with water until neutral pH. A solution of 1 g heparin in 45 ml deionized water was applied. The combined filtrate and washings were adjusted to pH 6.0 with pyridine. After solvent removal by evaporation, the product was lyophilized (Lyovac GT2, GEA, Düsseldorf, Germany). Subsequently, the pyridinium salt of heparin served as the starting compound for the N- and 6-O-desulfation procedure.

2.1.2. N-desulfation (N-DS) procedure [35]

25 ml DMSO containing 5% water was added to the pyridinium salt of heparin and the mixture was stirred for 1.5 h at 50 °C. After dilution with 25 ml water pH was adjusted to pH 9.5 with 1 N aqueous NaOH. The reaction mixture was dialyzed (MWCO = 8 kDa) against deionized water for 3 days, concentrated with a rotary evaporator (R-205, Büchi, Essen, Germany) and lyophilized with a freeze dryer (Lyovac GT2, GEA, Düsseldorf, Germany). To remove the resulting free amino group, which could possibly lead to heparin–heparin crosslinks upon carbodiimide-activation for gel formation, the product was subjected to N-acetylation procedure.

2.1.3. 6-O-desulfation (6-O-DS) procedure [34]

420 mg of the pyridinium salt of heparin was dissolved in 50 ml *N*-methyl-2-pyrrolidone containing 10% water. The reaction was carried out for 24 h at 90 °C. After cooling to room temperature 50 ml deionized water was added and pH adjusted to 9.0 by addition of 1 M aqueous sodium hydroxide. The reaction mixture was dialyzed (MWCO = 8 kDa) against deionized water for three days, concentrated with a rotary evaporator (R-205, Büchi, Essen, Germany) and lyophilized with a freeze dryer (Lyovac GT2, GEA, Düsseldorf, Germany). As this process additionally removes the *N*-sulfate, the product was subjected to the *N*-resulfation procedure to obtain exclusively 6-O-desulfated heparin.

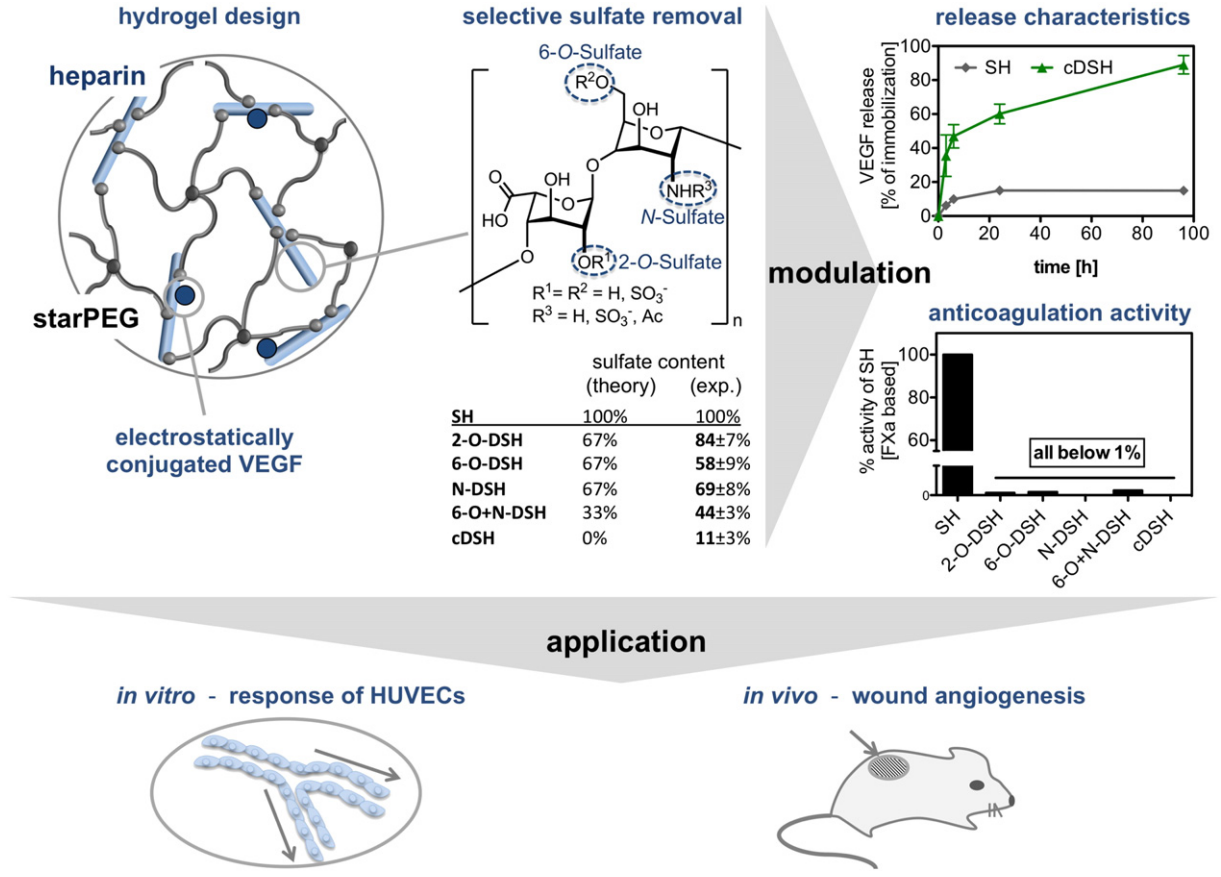

Fig. 1. Hydrogel design using selectively desulfated heparin derivatives as hydrogel building blocks. Overview of functional groups at 2-O, 6-O and N-position of heparin and its desulfated derivatives (2-O-DSH, 6-O-DSH, N-DSH, 6-O + N-DSH and cDSH), the corresponding theoretical sulfate content (assuming a desulfation efficiency of 100%) as well as the experimentally determined remaining sulfate content (mean ± standard deviation from n ≥ 3 for both polyelectrolyte titration and ATR–FTIR). Modulation of heparin release (exemplary shown for complete desulfated heparin, cDSH, see also Fig. 4B) and the anticoagulant activity (% activity compared to the activity of the standard heparin (SH), factor Xa based assay. Application of the hydrogels for endothelial cell response (human umbilical vein endothelial cells — HUVECs) and for wound healing in genetically diabetic (db/db) mice.

2.1.4. 2-O-desulfation (2-O-DS) procedure [33]

500 mg heparin was dissolved in 10 ml 0.4 M aqueous sodium hydroxide. The solution was frozen and lyophilized over night (Lyovac GT2, GEA, Düsseldorf, Germany). Dissolving and lyophilizing was done twice. The pH was adjusted to 9.0 with 20% acetic acid. After dialysis (MWCO = 8 kDa) against deionized water for three days the reaction mixture was concentrated and lyophilized.

2.1.5. N-acetylation (NAc) procedure [33]

20 ml 10% methanol containing 50 mM Na_2CO_3 was added to the reaction mixture. While stirring 200 μl acetic anhydride was added at 0 °C. The pH was adjusted to 7–8 with saturated Na_2CO_3 solution. Every 30 min 200 μl acetic anhydride was added for 3 h. The reaction mixture was dialyzed (MWCO = 8 kDa) against deionized water for 3 days, concentrated with a rotary evaporator (R-205, Büchi, Essen, Germany) and lyophilized with a freeze dryer (Lyovac GT2, GEA, Düsseldorf, Germany).

*Note: N-DS, 6-O-DS, 2-O-DS and NAc procedure were combined to obtain completely desulfated heparin (cDSH).

2.1.6. N-resulfation procedure [33]

200 mg *N*-desulfated heparin was dissolved in 40 ml water. 400 mg Na_2CO_3 and 400 mg trimethylamine-sulfur trioxide were added at room temperature. The mixture was stirred for 24 h at 55 °C. After cooling to room temperature, the reaction mixture was dialyzed (MWCO = 8 kDa) against deionized water for 3 days. The dialyzate was applied to a column of Amberlite IR-120 H^+-ion-exchange resin. The pH was adjusted to 9.5 with 0.1 M aqueous sodium hydroxide and dialyzed (MWCO = 8 kDa) against deionized water for 3 days, concentrated with a rotary evaporator (R-205, Büchi, Essen, Germany) and lyophilized with a freeze dryer (Lyovac GT2, GEA, Düsseldorf, Germany).

2.2. Characterization of desulfated heparin derivatives

2.2.1. Polyelectrolyte titration [36]

The anionic charge of the different heparin samples (unmodified and selectively desulfated heparin; 1 mg/ml in MilliQ, pH adjusted to 10) was determined by the Particle Charge Detector (PCD, Mütek GmbH, Herrsching, Germany) *via* titration with PDADMAC (poly(diallyldimethylammonium chloride)), respectively. Based on the exact charge compensation of the polyelectrolyte heparin by dropwise added PDADMAC solution (as indicated by streaming potential measurements), the titration of the heparin samples reveals a quantitative and reproducible estimation of its charges. To determine the heparin sulfate content, all the data were corrected for the charge contribution of the carboxylic acid group by subtracting one quarter of the overall charge of the non-desulfated heparin from all measured values (considering only the major sequence of heparin). Finally, the decrease of the anionic charge for the different desulfated heparins caused by the sulfate removal is expressed with respect to the non-desulfated heparin, which served as the control sample (sulfate content is set to 100%).

2.2.2. Infrared (IR) spectroscopy [30]

IR measurements on the different heparin samples (unmodified and selectively desulfated heparin; 1 mg/ml in MilliQ) were performed on an IFS 55 (EQUINOX, Bruker-Optics GmbH, Ettlingen, Germany) Fourier transform IR (FTIR) spectrometer in the attenuated total reflection (ATR) mode. The ATR–FTIR spectra were recorded on a special mirror setup using the "single-beam sample reference" concept. For that, the particular heparin solution was spread on the upper half (sample) of the silicon internal reflection element (50 × 20 × 2 mm^3) and the lower uncoated half was used as the reference. Shuttling the two halves repeatedly in the IR beam, recording the respective intensity spectra ($I_{Reference}(\nu)$, $I_{Sample}(\nu)$), and computing $A(\nu) = -\log(I_{Sample}(\nu) / I_{Reference}(\nu))$ resulted in well-compensated ATR–FTIR absorbance spectra ($A(\nu)$). For determination of the heparin sulfate content, the intensity peaks of the sulfate and the carboxylic acid group were recorded and their ratio was calculated. The decrease of this ratio for the different desulfated heparins indicated the sulfate removal, so that the remaining sulfate content could be determined with respect to the non-desulfated heparin, which served as the control sample (set to a sulfate content of 100%).

2.3. Preparation of starPEG-heparin hydrogels

StarPEG-heparin hydrogels –as well as gels made of starPEG and desulfated heparin derivatives– were formed by crosslinking amino end-functionalized four-arm starPEG (10,000 g/mol Polymer Source, Inc., Dorval, Canada) with EDC/s-NHS activated carboxylic acid groups of heparin or its desulfated derivatives [30]. A total polymer content of 11.76% and a 2:1:1 ratio of EDC:s-NHS:NH_2-groups of starPEG [mol/mol] were used. The molar ratio of starPEG to heparin (γ) was set to 3. To allow for cell-mediated remodeling of the matrix during the *in vivo* experiments, hydrogel scaffolds with adapted mechanical properties (γ = 2) were similarly produced using a starPEG conjugated to an MMP-cleavable peptide sequence [37].

For an application in different experimental setups, gels were formed as surface-bound networks with a final thickness of ~50 μm (3.13 μl gel mixture/cm^2 used for quantitative VEGF binding/release studies and *in vitro* cell culture experiments) as described in [38]. To allow for an introduction into the *in vivo* system, small free-standing hydrogel disks with a final thickness of ~2.5 mm were prepared by pipetting 13.68 μl of the gel mixture between two 5 mm hydrophobic glass cover slips treated with hexamethyldisilazane (Fluka, Seelze, Germany). After polymerization overnight at 22 °C, each gel sample was washed in phosphate buffered saline (PBS) to remove s-NHS/EDC and any non-bound starPEG/heparin [24]. For cell culture, sterilization was performed by UV-treatment for 30 min. For additional treatments, all solutions were sterile unless otherwise indicated.

2.4. Biomolecular functionalization of starPEG-heparin hydrogels

Functionalization with 2 μg/gel cyclo(Arg-Gly-Asp-D-Tyr-Lys) (RGD) peptide (Peptides International, Louisville, KY, USA) was performed as described in [24]. Briefly, heparin carboxylic acid groups of swollen hydrogels were activated with s-NHS/EDC solution (400 μl with 25 mM s-NHS and 50 mM EDC in 1/15 M phosphate buffer (pH 5)) for 45 min at 4 °C and subsequently incubated with RGD-solution (400 μl with 5 μg/ml RGD dissolved in borate buffer) for 2 h at room temperature. Finally, all samples were washed in PBS 3 times. To immobilize VEGF165 (PeproTech GmbH, Hamburg, Germany) to the starPEG-heparin networks, the respective protein was dissolved in PBS at the desired concentration (0.1, 1 or 5 μg/ml). PBS-swollen, pure or RGD-modified gels were immersed in this solution at room temperature for 24 h followed by rinsing twice with PBS.

2.5. Characterization of VEGF binding and release by Enzyme-Linked Immunosorbent Assay (ELISA)

Surface-bound gels (3.13 μl; n = 3) were placed in custom-made incubation chambers that allowed only minimal interaction of the protein solution with areas not originating from the hydrogel. 200 μl of VEGF (1 or 5 μg/ml) solution was added per cm^2. Immobilization was performed over night at 22 °C. The VEGF solution was removed followed by two washes with PBS. Each of these solutions was collected and assayed in duplicate using an ELISA Quantikine kit (R&D Systems, Minneapolis, USA). After immobilization, VEGF was allowed to release from these gels at 22 °C into 250 μl/cm^2 of serum-free (SF) endothelial cell growth medium (ECGM; Promocell GmbH, Heidelberg, Germany) supplemented with 0.02% ProClin 300 + 1 mg/ml bovine serum albumin (BSA). Samples were always taken at the same intervals (after 3, 6, 24 and

96 h) and stored at −80 °C until analyzed by ELISA. An equal volume of fresh medium was added back at each time point.

2.6. In vitro assays

2.6.1. Cell culture

Primary human umbilical vein endothelial cells (HUVECs), isolated according to the procedure proposed by Weis et al. [39], were cultured up to 80% confluence in medium containing supplement and 50 μg/ml of ascorbic acid (Lonza, Walkersville, USA).

2.6.2. Transwell assay

Hydrogels (3.13 μl) were formed at the bottom of 24-well plates. Upon overnight incubation with VEGF (1 or 5 μg/ml), hydrogels were briefly washed with PBS. Transwell filters (3 μm, Millipore) were coated with 50 μg/ml collagen type I in 0.02 acetic acid, washed twice with PBS and air-dried. The hydrogels were overlayed with 500 μl serum-free medium. Full medium was used a positive control. 2×10^5 HUVECs were seeded on each membrane is serum-free medium and cultured for 6 h. Afterward, cells were fixed with 2% PFA for 15 min, following by 30 min cell staining with 0.1% crystal violet in 20% methanol. Excess of dye was washed off with several changes of distilled water. The non-migrated cells on the upper side of the membrane were scraped off with cotton tabs and the membranes were air-dried over night. The membranes were photographed with microscope (Olympus IX50, 20× objective). The extent of cell migration was quantified by dye-staining the cells on the filters with 10% acetic acid and measuring the intensity of the dye at 590 nm with TECAN Genios plate reader. Subsequently, the dye intensity was normalized to the intensity of positive control (full medium).

2.6.3. Collagen overlay

Hydrogels (3.13 μl) were formed at the bottom of 48-well plate. Upon overnight incubation with VEGF (1 or 5 μg/ml), hydrogels were briefly washed with PBS and overlaid with 200 μl of 2.5 mg/ml collagen type I solution (BD Pharmingen, Heidelberg, Germany). The collagen gels were allowed to polymerize at 37 °C for 1 h. Before cell seeding, hydrogels were equilibrated in 300 μl of ECGM for 1 h at 37 °C. HUVECs were seeded at the collagen gels in the amount of 2×10^5/well and cultured for 3 days. Finally, samples were fixed with 3% glutaraldehyde and subjected to light microscopy (Olympus IX50, 10× objective, Hamburg, Germany). ImageJ software (developed by W. Rasband, National Institutes of Health, Bethesda, USA) was used to quantify the length of tubular structures. The results were shown as mean tube density (mm/mm^2) ± SEM.

2.6.4. Immunostaining

Samples were stained with Phalloidin CF488 (Biotum, Hayward, USA). The images were taken with confocal microscope (SP5, Leica Microsystems, Bensheim, Germany; 20×/0.70 objective).

2.7. Anticoagulant activity

The anticoagulant activity of the desulfated heparins was determined in an FXa based heparin assay (Chromogenix, Milano, Italy). The modified heparins were added to citrate plasma and their anti-FXa activity was rated to the activity of native heparin.

The coagulation time of recalcified citrate plasma was determined using the fluorogenic thrombin substrate ZGGR-AMC (Technothrombin SUB, Technoclone, Vienna, Austria) in the presence of phospholipids (Technothrombin RA), the activator dextran sulfate (1 μg/ml, MW 500 kDa, Sigma-Aldrich) and the test-heparins up to 170 μg/ml. The fluorescence was followed at λex = 360 nm, λem = 465 nm (Tecan Genios, Tecan, Männedorf, Switzerland) and the time point of an increase of 200 fluorescent units was defined as coagulation time.

2.8. In vivo wound healing assay

2.8.1. Excisional wounding and VEGF treatment in mice

Animal experiments were performed in accordance with the animal ethics guidelines of the German law. Wounding of diabetic mice was performed as previously described [9,40]. Briefly, backs of BKS.Cg-m +/+ $Lepr^{db}$/J (db/db) mice (Charles River Laboratories, Wilmington, MA, USA) (male, 12–14 weeks of age, n = 20 mice in total) were shaved and four full-thickness punch biopsy wounds per mouse were created enabling for simultaneous testing of 4 different conditions per mice.

In the first experiment, hydrogels formed of SH of different stiffness with soft (storage modulus ≈2 kPa) and hard (storage modulus ≈6 kPa) hydrogels incubated with vehicle (PBS) or the hard gel with VEGF (1 μg) (conditions 1–3) and pure PBS (no hydrogel) (condition 4) were tested (n = 10 mice with four wounds, i.e. 20 wounds at every timepoint). In the second experiment, hydrogels prepared from cDSH incubated with vehicle (PBS) or VEGF protein (0.1 μg or 1 μg) (conditions 1–3) were placed into the wound site, plus one wound with PBS alone (no hydrogel, condition 4) (n = 10 mice with four wounds, i.e. 5 mice with 20 wounds at every timepoint). To avoid drying of the gel, the wound was covered with a non-adhering gauze (Adaptic®, J&J Norderstedt, Germany) and a semipermeable foil (Hydrofilm®, Hartmann, Heidenheim, Germany). At day 10 or 15, mice were sacrificed and the wound tissue was harvested for histological analysis. When the semipermeable wound cover was lost during the experiment, some wounds could not be evaluated for technical reasons.

2.8.2. Histology and immunohistochemistry

Wound tissue was excised and either fixed overnight in 4% paraformaldehyde in PBS, or embedded in Tissue-Tek OCT compound (Sakura Finetek, Alphen aan den Rijn, The Netherlands), immediately frozen in liquid nitrogen, and stored at −80 °C. Cryosections were stained with hematoxylin/eosin or for immunohistochemical analysis were fixed in acetone, unspecific binding sites were blocked with 3% BSA, and sections were incubated with polyclonal rat antisera against murine CD31 (BD Pharmingen), monoclonal rat antisera against murine Gr-1 (BD Pharmingen), monoclonal rat antisera against murine F4/80 (Dianova, Hamburg, Germany), or monoclonal Cy3 conjugated mouse antisera against aSMA; bound primary antibody was detected using an Alexa Fluor 488-conjugated polyclonal goat anti-rat antibody (Molecular Probes, Invitrogen, Paisley, UK) or HRP conjugated polyclonal goat anti-rat antibody (Southern Biotech, Birmingham, USA). As a control for specificity, primary antibodies were omitted and replaced by irrelevant isotype-matched antibodies.

2.8.3. Morphometric analysis

Immunofluorescence/immunohistochemical microscopy was conducted at indicated magnifications (Microscope Eclipse 800E; Nikon, Melville, USA). Morphometric analysis was performed on digital images using the Imaging Software Lucia G 4.80 (Laboratory Imaging Ltd., Prague, Czech Republic). The extent of epithelization and granulation tissue formation was determined on hematoxylin/eosin (H&E)-stained tissue sections as previously described [9,40]. For quantitative analysis of vascular structures, the area that stained positive for CD31 within the granulation tissue was calculated.

2.9. Statistical analysis

Statistical significance was calculated using the GraphPadPrism 5 or GraphPad InStat software package (La Jolla, USA) and accepted for $p < 0.05$ ($^*p < 0.05$, $^{**}p < 0.01$, $^{***}p < 0.001$, $^{****}p < 0.0001$). Data was analyzed by the paired or unpaired Student's t-test or by One-way ANOVA analysis followed by appropriate post-tests. For the *in vivo* experiments with n ≥ 3 p values were of explorative character.

3. Results and discussion

3.1. Desulfation of heparin

Defined desulfated heparin (DSH) derivatives were obtained by applying previously described procedures targeting for the 2-O-, 6-O- and N-sulfate groups of the unmodified (fully sulfated) heparin (SH) [41, 33–35]. Fig. 1 summarizes the resulting derivatives and gives their expected sulfate contents as well as the experimentally determined values. Quantification was based on averaging data from both polyelectrolyte titration and ATR–FTIR spectroscopy [30]. Generally, the applied methods led to an effective desulfation of more than 80% in agreement with published procedures. Interestingly, all desulfated derivatives showed an anticoagulant effect of less than 1% compared to SH, measured as anti-FXa–activity, see Fig. 1. The desulfated heparins also did not delay the coagulation time of recalcified citrate plasma, indicating that the whole coagulation cascade was not affected (data not presented). This points to the fact that the rare 3-O sulfate necessary for effective thrombin inactivation [31,32] is removed independently of the particular desulfation procedure. Thus, all desulfated derivatives should not cause any hemorrhagic side effects.

Following a mean-field based approach to modulate mechanical properties and sulfation patterns of biohybrid hydrogels independently [30], hydrogels with graded sulfation pattern, desulfated at 2-O, 6-O, N-position, 6-O and N as well as 2-O, 6-O and N-position (complete sulfate removal) were synthesized (see Fig. 1). The resulting hydrogels were used to study the influence of a particular sulfate group (2-O, 6-O or N, Section 3.2), the overall sulfate content (ranging from 100 to ~10% residual sulfate content, Section 3.3), the growth factor loading concentration (Section 3.4) to the subsequent release of the protein. Furthermore, the pro-angiogenic effects of the modulated VEGF release from the different hydrogels was analyzed *in vitro* (Section 3.5) and *in vivo* (Section 3.6) (see Fig. 1).

3.2. Influence of the sulfate position on VEGF delivery

Since the meshsize of the hydrogels in the range of 8–10 nm (according to the rubber elasticity theory for the 6–8 kPa stiff hydrogels, see [30]) is large enough compared to the size of VEGF with an hydrodynamic diameter of ~6 nm [42], the VEGF diffusion throughout the matrices shall be predominantly determined by the affinity of the protein to the particular sulfated heparin derivative and not by the mesh size of the hydrogel that is underpinned by earlier results of similar VEGF delivery out of different stiff hydrogels using the sulfated heparin as building block [26].

As VEGF preferentially interacts with 6-O- and N-sulfate groups of heparin, while nevertheless also the 2-O-sulfate and the carboxylic acid residues contribute to the overall binding strength [29,43], it was determined whether the conjugation of VEGF within the starPEG-heparin hybrid networks is similarly influenced. As indicated in Fig. 2A, the removal of only one sulfate group within starPEG-heparin gels did not show any effect on the uptake of 1 μg/ml VEGF (200 μl/cm^2 gel). For gels formed out of SH, 2-O-, 6-O- or N-DSH, a comparable binding efficiency of ~93% ($p > 0.05$, ANOVA) was determined 24 h after contact with the protein solution. The origin for this interesting behavior is most likely due to the high heparin content of the hydrogels with two remaining sulfate groups per disaccharide unit being sufficient for efficient protein binding.

Considering the cumulative release of VEGF (Fig. 2B), similar kinetics were observed for all hydrogels formed out of the different heparin derivatives showing a comparable initial burst release within the first 6 h. Such burst characteristics are often attributed to surface effects [44] and could be caused by a VEGF fraction entrapped in the meshwork but not specifically bound to heparin. However, after 24 h, the release continued slowly over the course of the entire time period that was investigated, indicating the potential of the materials for applications with a need for long-term delivery profiles of growth factors.

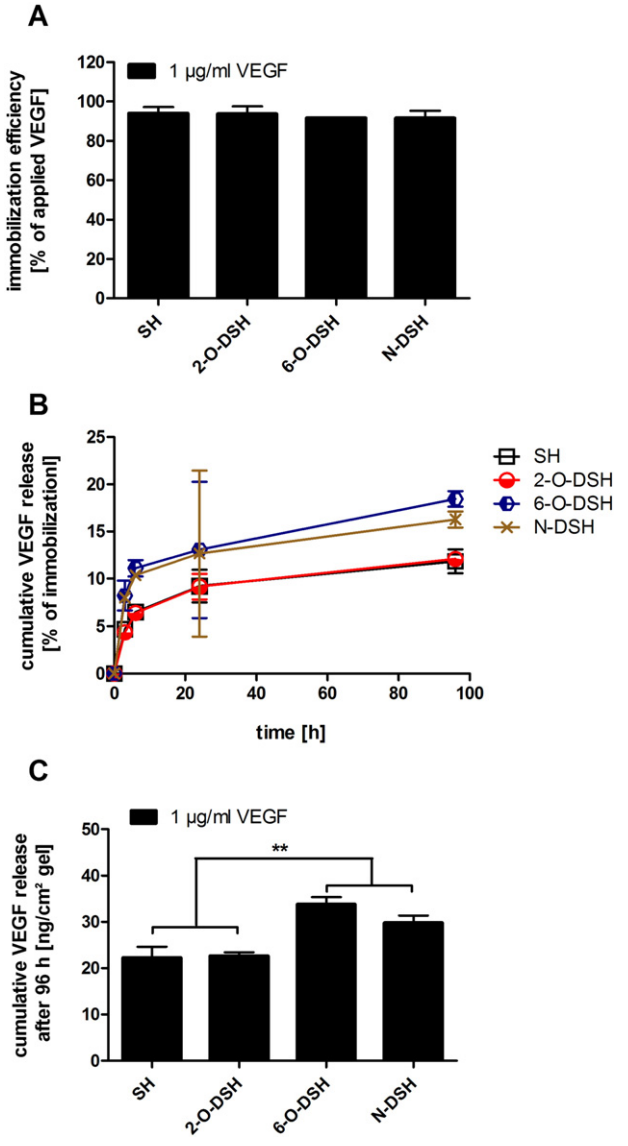

Fig. 2. Influence of the specific sulfate removal on the VEGF delivery by starPEG-heparin hydrogels prepared from selectively desulfated heparin derivatives. 2A: Immobilization efficiency expressed as % of applied VEGF. 2B: Cumulative VEGF release expressed as % percent of immobilization (release kinetics). 2C: Cumulative VEGF release after 96 h expressed as ng/cm^2 gel (absolute quantities).

However, besides the overall similar shape of the curves, nevertheless different amounts of VEGF were sequestered (Fig. 2C) within 96 h. Compared to SH (release of ~22 ng VEGF/cm^2 gel; 12% of immobilized amount) and 2-O-DSH (release of ~23 ng VEGF/cm^2 gel; 12% of immobilized amount), the growth factor release could be significantly increased ($p < 0.01$, ANOVA) by using 6-O-DSH (release of ~34 ng VEGF/cm^2 gel; 18% of immobilized amount) or N-DSH (release of ~30 ng VEGF/cm^2 gel; 16% of immobilized amount) as gel building block. Since the immobilization of VEGF was hardly affected by the removal of a single sulfate group (see discussion above), the growth factor release efficiency (calculated as % released after 96 h normalized to the VEGF amount used for hydrogel loading) was similar to the release normalized to the immobilized amount, for SH: 11% vs. 12%, for 2-O-DSH: 11% vs. 12%, for 6-O-DSH: 17% vs. 18% and for N-DSH: 15% vs. 16%. In contrast to the initial binding, upon larger time scales with repeated exchange of the release medium, analysis of the delivery clearly shows the decisive role of these two key sulfate groups mediating the affinity between VEGF and heparin [29,43], whose removal substantially weakens the interaction of the growth factor with the hydrogel.

Consequently, the provision of VEGF could be specifically modulated by incorporation of 6-O-DSH or N-DSH into starPEG-heparin scaffolds, where unaffectedly high binding efficiencies going along with nevertheless increased release rates were achieved.

3.3. Influence of the overall sulfate content on VEGF delivery

Besides the influence of a specific sulfate position, it was determined that a variation of the overall sulfate content (see Fig. 1) could be applied to modulate VEGF delivery by starPEG-heparin hydrogels.

As previously discussed (3.2), the removal of the *N*-sulfate (~ 70% sulfate remaining, see Fig. 1) did not influence the uptake of 1 μg/ml VEGF (200 μl/cm^2 gel) compared to hydrogels formed out of SH (unmodified sulfate content of 100%). However, a successive decrease of the sulfation degree to ~44% upon elimination of both the 6-O- and N-sulfate as the key interaction sites for VEGF, the growth factor binding efficiency was reduced to ~67% of applied protein ($p < 0.05$, ANOVA, see Fig. 3A). Interestingly, although an additional removal of the 2-O-sulfate to obtain cDSH even decreased the remaining sulfate content down to ~11%, the lack of this particular residue, which is not considered to mediate the VEGF affinity to heparin, did not result in a further reduction of the binding efficiency (~73%). Here, the large protein uptake, despite the low sulfation degree, might be due to the overall high heparin content of the hydrogels (~2000× molar excess compared to VEGF), thereby still offering a substantial amount of VEGF binding sites for a rather effective immobilization of the growth factor.

For the release kinetics (Fig. 3B), upon successive removal of the sulfate groups, the burst effect became slightly more pronounced as indicated by the initial steep incline of the corresponding curves. Independently of the particular sulfate content, after the burst release a continuous (slow) release of VEGF was determined over the course of 96 h. As expected, the overall amount of sequestered VEGF (Fig. 3C) was found to be significantly influenced by the sulfate content of starPEG-heparin hydrogels. As discussed in Section 3.2 for N-DSH (~70% sulfate remaining), even the lack of one residue involved in VEGF interaction with heparin significantly enhanced the protein release compared to SH. Similarly to the binding studies, this effect could be increased further by removing both the 6-O- and N-sulfate leading to a sulfation degree of only ~44% (release of ~41 ng VEGF/cm^2 gel; 31% of immobilized amount, $p < 0.01$, ANOVA). Starting from these elevated levels, an additional elimination of the 2-O-sulfate for cDSH giving ~11% sulfate remaining could not further enhance the release efficiency (release of ~42 ng VEGF/cm^2 gel; 29% of immobilized amount). Noteworthy, although lower amounts of VEGF

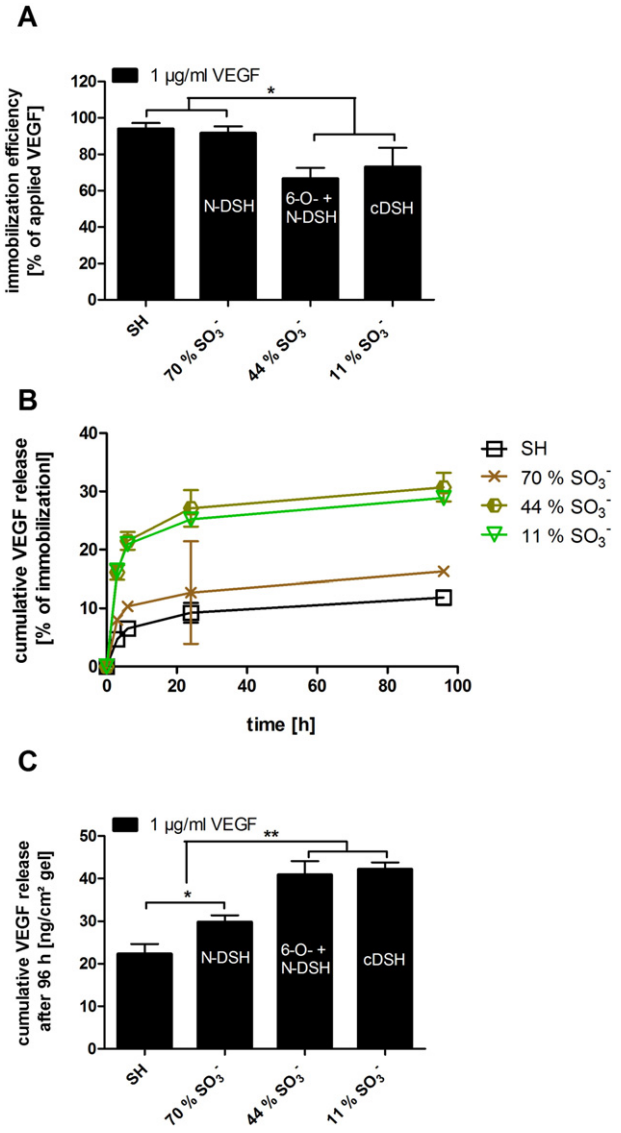

Fig. 3. Influence of the overall sulfation degree on the VEGF delivery by starPEG-heparin hydrogels prepared from selectively desulfated heparin derivatives. 3A: Immobilization efficiency expressed as % of applied VEGF. 3B: Cumulative VEGF release expressed as % percent of immobilization (release kinetics). 3C: Cumulative VEGF release after 96 h expressed as ng/cm^2 gel (absolute quantities).

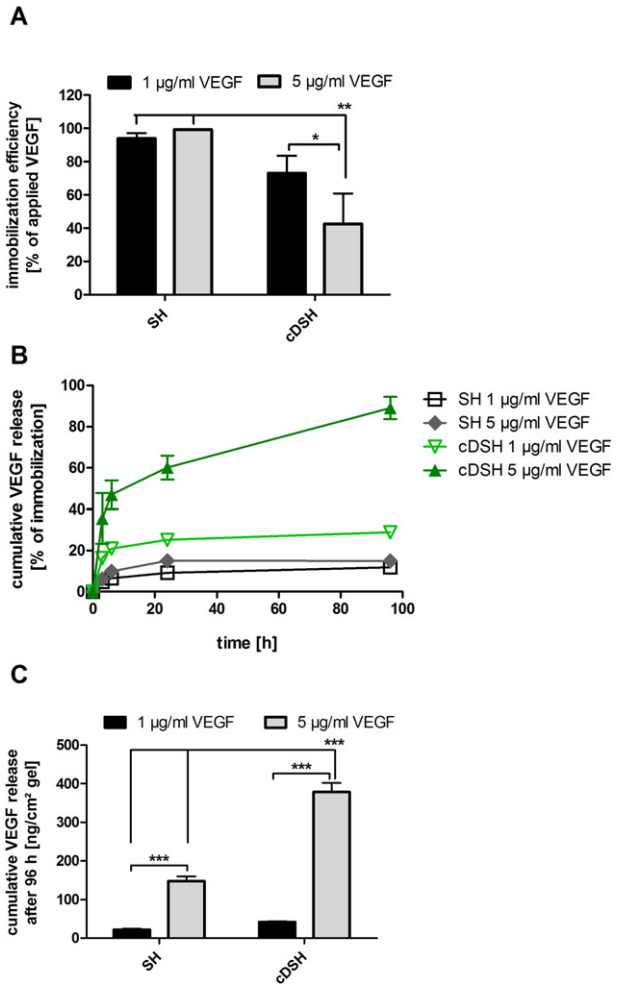

Fig. 4. Influence of the protein concentration on the VEGF delivery by starPEG-heparin hydrogels prepared from selectively desulfated heparin derivatives. 4A: Immobilization efficiency expressed as % of applied VEGF. 4B: Cumulative VEGF release expressed as % percent of immobilization (release kinetics). 4C: Cumulative VEGF release after 96 h expressed as ng/cm^2 gel (absolute quantities).

were immobilized with decreasing sulfate content, the absolute quantities of growth factors being released could be gradually elevated.

Furthermore, the release efficiency (calculated as % released after 96 h normalized to the VEGF amount used for hydrogel loading) is increased: SH (100% sulfation): 11%, N-DSH (70% sulfation): 15%, 6O- + N-DSH (44% sulfation): 20% and cDSH (11% sulfation): 21%. Consequently, the amount of VEGF available for delivery after immobilization to the desulfated hydrogels can be adjusted to the particular requirements of a certain application. Moreover, a further so-far-unexplored advantage of this system could be a decreased re-binding of hydrogel released growth factors and a reduced scavenging of cell-secreted soluble effectors.

In sum, the delivery of VEGF by starPEG-heparin hydrogels can be gradually tuned by targeted removal of specific sulfate residues that mediate the heparin affinity of the particular growth factor (6O- and N-sulfate in case of VEGF).

3.4. Influence of the loading concentration to the VEGF delivery

While the VEGF delivery was found to be adjustable upon changing the type and content of its sulfate binding residues within the building blocks for starPEG-heparin hydrogels, it was additionally analyzed whether hydrogels with substantially reduced numbers of interactions sites (cDSH with only ~11% sulfate groups remaining) are still applicable to administer larger concentrations of the growth factor (5 μg/ml).

For hydrogels prepared from SH (Fig. 4A), the factor concentration used for loading did not affect the immobilization efficiency (~97%, $p > 0.05$, ANOVA). However, when cDSH was incorporated into the scaffolds, the VEGF uptake of ~73% (1 μg/ml protein) was further reduced to ~43% when five times more growth factor was applied ($p < 0.05$, ANOVA), indicating that the decreased number of available binding sites for this derivative becomes a limiting factor in immobilizing higher amounts of VEGF. However, considering a loading of 200 μl protein solution per cm^2 gel, binding efficiencies would result in ~150 ng VEGF/cm^2 for 1 μg/ml and ~430 ng VEGF/cm^2 for 5 μg/ml. Thus, the uptake of VEGF is still adjustable over a large range and might be sufficient to promote a certain cell response, as growth factors already elicit their biological function when present at pico- or nanomolar concentrations [45].

The release kinetics of VEGF are strongly influenced for an application of 5 μg/ml protein and the usage of cDSH as a starPEG-heparin hydrogel building block (Fig. 4B). Here, compared to all other conditions, a steeper incline (i.e. faster release) at any time point is due to less available protein binding sites and therefore less efficient rebinding to the hydrogel matrix. Similarly, the overall quantity of sequestered VEGF is affected (Fig. 4C). For incorporation of unmodified SH into the gels, a five times higher protein concentration in the loading solution resulted in increased absolute amounts of VEGF being released (release of ~148 ng VEGF/cm^2 gel, $p < 0.001$, ANOVA), but considering the similar factor uptake, to a similar percentage of release and release efficiencies (~12–15%) as for 1 μg/ml VEGF (see similar curves in Fig. 4B). When cDSH is applied as a hydrogel building block, 5 μg/ml VEGF also led to higher absolute quantities being sequestered (release of ~379 ng VEGF/cm^2 gel) when compared to a five times lower protein concentration ($p < 0.001$, ANOVA). Moreover, due to a lower initial binding efficiency, different than for 1 μg/ml VEGF (see dissimilar curves in Fig. 4B), almost all growth factor was released within 96 h (89% of immobilized amount). Additionally, a further increased release efficiency of up to 38% of the initially for the loading applied VEGF amount after 96 h was found for this particular setting (5 μg/ml VEGF loaded to cDSH-based gels).

Overall, the adjustment of sulfation degree in combination with different loading concentrations advantageously allows for tuning the uptake and release of growth factors to/from the hydrogel matrices, both with respect to the release kinetics and the released amounts(Supplementary Fig. 2).

3.5. Endothelial cell response to hydrogel based VEGF gradients

VEGF is known for its multiple effects at the wound healing process including the promotion of angiogenesis, epithelization and collagen formation [3]. The pro-angiogenic action of VEGF results in chemotactic

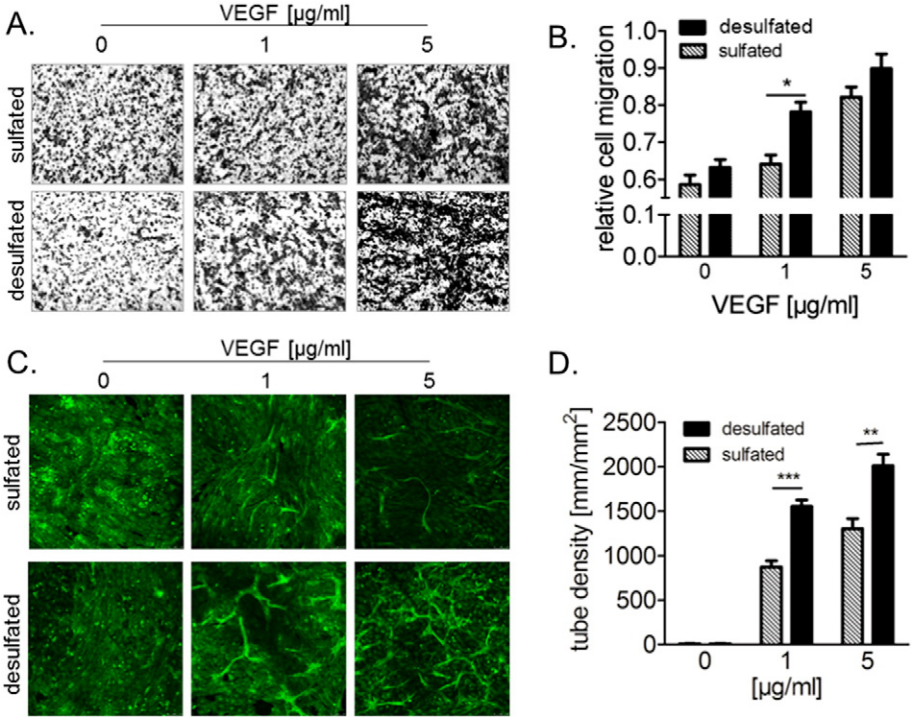

Fig. 5. Endothelial cell response to hydrogel released VEGF. A) Cell migration through the membranes depicted with crystal violet staining after 6 h culture. B) Quantified relative cell migration as normalized to the positive control. C) Endothelial cell morphogenesis on a collagen I/star-PEG-heparin gel sandwich visualized with phalloidin staining after 3 days culture. D. Quantification of the tube length of HUVECs on collagen I/starPEG-heparin gel sandwich after 3 days culture.

endothelial cell migration, proliferation, ECM invasion and new blood vessel formation [3]. Therefore, the effect of VEGF gradients established from SH and cDSH hydrogels immobilized at the bottom of 24 well plates loaded with either 0, 1, or 5 μg/ml growth factor has been investigated. Cell migration was analyzed by culturing the cells on transwell-inserts coated with collagen type I as endothelial cell migration is primarily mediated through integrin binding to the ECM [46] (Fig. 5A and B). The cell migration was enhanced in the presence of VEGF-releasing cDSH-hydrogels as compared to the empty hydrogels (Fig. 5A). Importantly, the amount of migrating cells was higher in the presence of desulfated heparin (cDSH) hydrogels due to the higher released VEGF amount (Fig. 4). A significant difference in the number of migrating cells was found for hydrogels loaded with 1 μg/ml growth factor, but was less obvious for 5 μg/ml loading (Fig. 5B). The migratory response of endothelial cells to the administration of VEGF is known to be concentration-dependent with a plateau of the effect observed at higher concentrations [47]. This suggests that endothelial cell migration reached a plateau due to the high VEGF release from both types of hydrogels loaded with 5 μg/ml of protein, thus resulting in a smaller difference between the SH and cDSH heparin.

To evaluate the response of endothelial cell to VEGF delivered across tightly packed ECM meshworks as, for example, in wound healing, we overlaid VEGF-loaded hydrogels with a thick, fibrillar collagen type I layer prior to cell seeding (Fig. 5C and D). Accordingly, there was no direct contact of the HUVECs with the starPEG-heparin matrix. Upon 3 days of culture, morphogenesis of endothelial cells was observed for both types of SH and cDSH hydrogels releasing VEGF as indicated by the formation of tubular structures at the collagen surface (Fig. 5C and

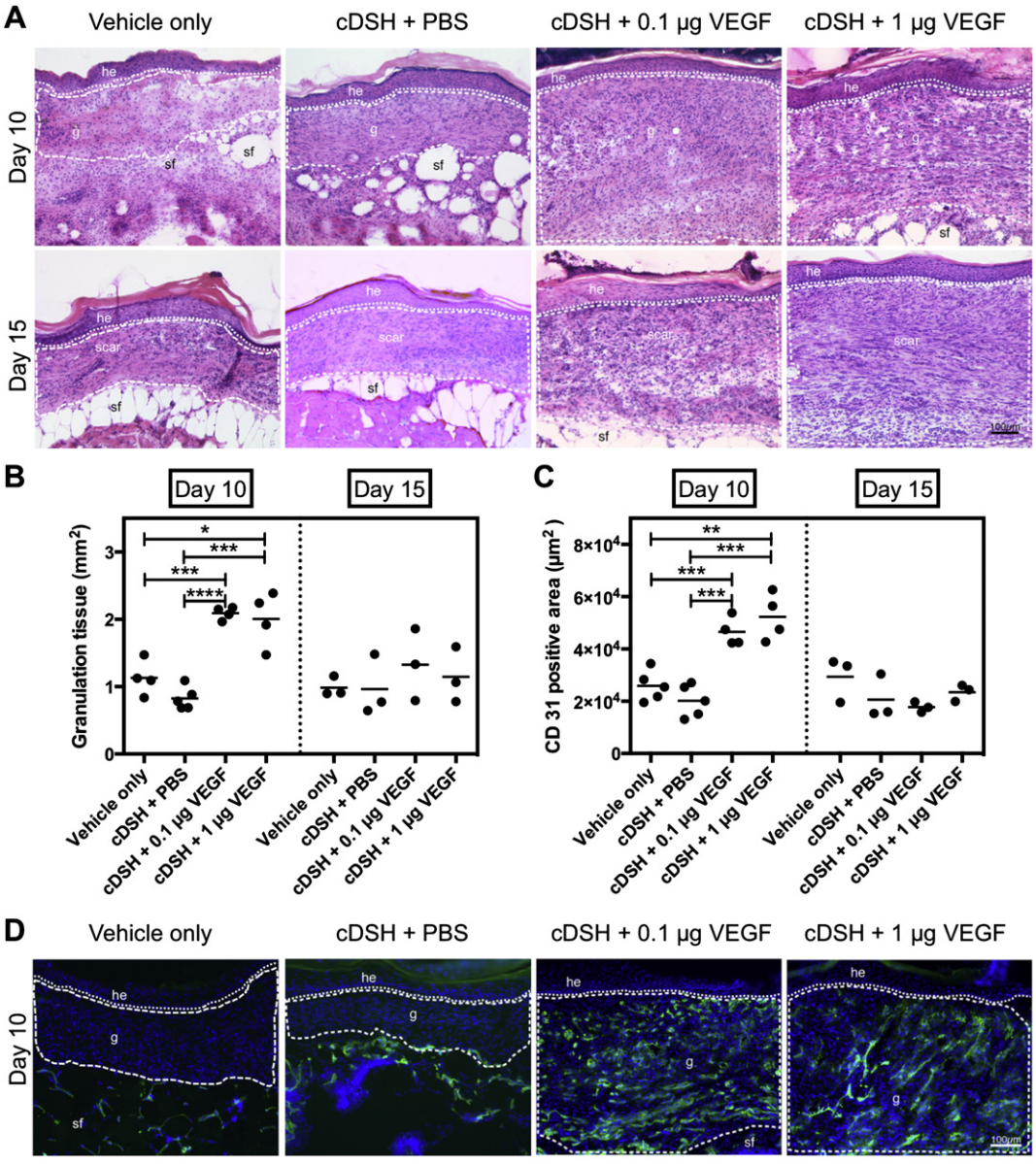

Fig. 6. cDSH-based hydrogels containing VEGF promote wound angiogenesis in diabetic mice. A) Representative H&E stainings (cryosections) of wounds, 10 and 15 days post injury, treated with vehicle only, cDSH + PBS, cDSH based hydrogels loaded with different amount of VEGF as indicated; granulation tissue in cDSH + VEGF treated wounds is characterized by high vascularization and cellularity and is covered by a hyperproliferative and closed epithelium; in vehicle only or cDSH + PBS treated wounds limited granulation tissue developed over the subcutaneous fat; scale bar: 100 μm. B) Morphometric quantification of granulation tissue. C) Morphometric quantification of blood vessels (CD31 stain) within granulation tissue of differentially treated wounds as indicated. D) CD31 (green) stained cryosections of day 10 wounds treated as indicated; DAPI counterstaining of nuclei (blue); scale bar: 100 μm. Each point represents a different wound tissue in a different mice; he, hyperproliferative epidermis; g, granulation tissue; sf, subcutaneous fat tissue; dotted line, indicates basement membrane; dashed line outlines granulation tissue (day 10)/scar tissue (day 15).

D). Morphogenesis of HUVECs on the collagen I/starPEG-heparin sandwich was observed to be VEGF dose-dependent and did not take place in the absence of VEGF, independent of the hydrogel type (Fig. 5C and D). Tubular structure density was significantly higher when the cDSH heparin was used at both 1 and 5 μg/ml loaded growth factor and in good agreement with the total released amount (Fig. 4C) indicating that increased VEGF release due to the desulfation results in more pronounced angiogenic cell response *in vitro*.

3.6. VEGF-releasing hydrogels promotes wound angiogenesis in diabetic mice

Vascular growth is essential for effective tissue repair and is profoundly attenuated in the preclinical model of impaired healing such as the diabetic db/db mouse [40,48,8]. Full thickness excision skin wounds were created on the back of diabetic mice and the repair response was characterized following a single, local treatment of wounds with hydrogels formed out of SH or cDSH preloaded with/without VEGF.

In a first experiment, soft and hard hydrogels based on SH, a hard hydrogel loaded with 1 μg VEGF per wound, and vehicle only (untreated, no gel) treated wounds were investigated. The results show, that for both time points (days 10 and 15 post injury) the wound tissue was hemorrhagic (soft gel) or the hydrogel was not invaded by cells (hard gel) (Supplementary Fig. 1). In view of the excellent (low) anticoagulant activity (see Section 3.1), a widely tuneable VEGF release (Sections 3.3 and 3.4) as well as a superior *in vitro* response of HUVECs to the modulated VEGF release (Section 3.5) of cDSH based hydrogels, the second *in vivo* study included those hydrogels only. Thus, vehicle only (PBS, no gel), cDSH based hydrogels loaded with PBS or with different amounts of VEGF (0.1 μg or 1 μg per gel) were transplanted and wound assessment was performed after 10 and 15 days post injury, and representative wound histologies for the different treatment conditions are shown (Fig. 6).

Analysis of H&E-stained cryosections of wound tissue revealed that at day 10 post injury in all conditions the hydrogel has been resolved and replaced by granulation tissue that was covered by a hyperproliferative neo-epithelium (Fig. 6A). Quantitative assessment revealed that the extend of granulation tissue was significantly increased when cDSH based hydrogels were pre-loaded with VEGF in comparison to cDSH based hydrogels loaded with PBS or for vehicle only treated wounds (Fig. 6B). The granulation tissue that developed in the presence of cDSH based hydrogels containing VEGF was characterized by a pronounced vascular response and increased cellularity when compared to wound tissue treated with cDSH hydrogels loaded with PBS or for vehicle only treated wounds (Fig. 6A). Staining for polymorphonuclear cells (Gr-1), macrophages (F4/80) and myofibroblasts (aSMA-actin) revealed a similar density of abundant macrophages and myofibroblasts within the granulation tissue of VEGF and vehicle loaded hydrogels, whereas polymorphonuclear cells were absent in all conditions (data not shown). At high magnification, erythrocytes were detected in the vessel lumen in VEGF-treated granulation tissue indicating the functionality and integrity of the vascular structures. Quantitative analysis of vascular structures by CD31 staining on cryosections showed that PBS (vehicle only) or the unloaded hydrogels (cDSH + PBS) had little effect on wound angiogenesis over the entire time course of healing (Fig. 6C and D). In contrast, granulation tissue that developed in the presence of hydrogel preloaded with VEGF was characterized by a significantly increased vascular response at day 10 post injury. Notably, at both concentrations of VEGF the induction of capillaries was significantly increased when compared to controls. At day 15 post injury, the density of VEGF-induced vascular structures within the scar tissue declined, indicating a timely limited angiogenic response (Fig. 6C).

Collectively, our findings prove that the degree of heparin sulfation in starPEG-heparin hydrogels are critical for obtaining an optimal set of low anticoagulant behavior and high VEGF release (see Fig. 1) and is therefore suitable to promote soft tissue growth (Fig. 6). Furthermore, we demonstrate that VEGF, a master regulator of angiogenesis, can be integrated and protected *via* the supportive starPEG-heparin hydrogel matrix to promote the vascularization of the developing connective tissue in diabetic impaired healing conditions.

3.7. Conclusion

Interactions of VEGF with starPEG-heparin hydrogels were successfully modulated by selective desulfation of the heparin unit. Specific removal of single sulfate groups mediating protein-GAG affinity (6-O- or N-sulfate) resulted in higher VEGF release rates at unaffected uptake levels. Removal of both 6-O- or N-sulfate moieties or loading of increased VEGF amounts reduced the growth factor binding efficiency but enabled the delivery of higher amounts of the cytokine. Removal of 10% of the sulfate groups of heparin was shown to be sufficient to reduce the anti-coagulant activity of below 1%.

Hydrogels formed out of cDSH were concluded to be superior with respect to efficacy of VEGF administration, a low anticoagulant activity and for the promotion of therapeutic angiogenesis.

Supplementary data to this article can be found online at http://dx.doi.org/10.1016/j.jconrel.2015.10.028.

Acknowledgments

This work was supported by the Deutsche Forschungsgemeinschaft through CRC TR 67 (UF, CW), WE 2539-7 (CW), CRC 829 (SAE), and FOR/EXC999 (CW), by the Leibniz Association (SAW-2011-IPF-2 68, CW), and by the European Union through the Integrated Project ANGIOSCAFF (CW). AZ was supported by a stipend of the Dresden International Graduate School for Biomedicine and Bioengineering. Contributions by Anika Röhrich (Center for Molecular Bioengineering B CUBE at TU Dresden) to the synthesis of selectively desulfated heparins, by Martin Müller (IPF Dresden) to characterization of the selectively desulfated heparins and Michael Piekarek (University of Cologne) for *in vivo* data evaluation are gratefully acknowledged.

References

[1] P.S. Briquez, J.A. Hubbell, M.M. Martino, Extracellular matrix-inspired growth factor delivery systems for skin wound healing, Adv. Wound Care 8 (2015) 479–489, http://dx.doi.org/10.1089/wound.2014.0603.
[2] S. Barrientos, H. Brem, O. Stojadinovic, M. Tomic-Canic, Clinical application of growth factors and cytokines in wound healing, Wound Repair Regen. 22 (2014) 569–578, http://dx.doi.org/10.1111/wrr.12205.
[3] P. Bao, A. Kodra, M. Tomic-Canic, M.S. Golinko, H.P. Ehrlich, H. Brem, The role of vascular endothelial growth factor in wound healing, J. Surg. Res. 153 (2009) 347–358, http://dx.doi.org/10.1016/j.jss.2008.04.023.
[4] S. Willenborg, T. Lucas, G. van Loo, J.A. Knipper, T. Krieg, I. Haase, et al., CCR2 recruits an inflammatory macrophage subpopulation critical for angiogenesis in tissue repair, Blood 120 (2012) 613–625, http://dx.doi.org/10.1182/blood-2012-01-403386.
[5] R.D. Galiano, O.M. Tepper, C.R. Pelo, K.A. Bhatt, M. Callaghan, N. Bastidas, et al., Topical vascular endothelial growth factor accelerates diabetic wound healing through increased angiogenesis and by mobilizing and recruiting bone marrow-derived cells, A.J.P. 164 (2004) 1935–1947, http://dx.doi.org/10.1016/S0002-9440(10)63754-6.
[6] C. Bauters, T. Asahara, L.P. Zheng, S. Takeshita, Site-specific therapeutic angiogenesis after systemic administration of vascular endothelial growth factor, J. Vasc. Surg. 21 (1995) 314–325.
[7] S. Takeshita, L.Q. Pu, L.A. Stein, A.D. Sniderman, S. Bunting, N. Ferrara, et al., Intramuscular administration of vascular endothelial growth factor induces dose-dependent collateral artery augmentation in a rabbit model of chronic limb ischemia, Circulation 90 (1994) II-228–II-234.
[8] D. Roth, M. Piekarek, M. Paulsson, H. Christ, W. Bloch, T. Krieg, et al., Plasmin modulates vascular endothelial growth factor-a-mediated angiogenesis during wound repair, Am. J. Pathol. 168 (2006) 670–684, http://dx.doi.org/10.2353/ajpath.2006.050372.
[9] S. Traub, J. Morgner, M.M. Martino, S. Höning, M.A. Swartz, S.A. Wickström, et al., The promotion of endothelial cell attachment and spreading using FNIII10 fused to VEGF-A165, Biomaterials 34 (2013) 5958–5968, http://dx.doi.org/10.1016/j.biomaterials.2013.04.050.
[10] D.R. Yager, S.M. Chen, S.I. Ward, O.O. Olutoye, R.F. Diegelmann, I. Kelman Cohen, Ability of chronic wound fluids to degrade peptide growth factors is associated

with increased levels of elastase activity and diminished levels of proteinase inhibitors, Wound Repair Regen. 5 (1997) 23–32.
[11] G. Lauer, S. Sollberg, M. Cole, I. Flamme, J. Stürzebecher, K. Mann, et al., Expression and proteolysis of vascular endothelial growth factor is increased in chronic wounds, J. Investig. Dermatol. 115 (2000) 12–18, http://dx.doi.org/10.1046/j.1523-1747.2000.00036.x.
[12] Y.H. Kusumanto, V. van Weel, N.H. Mulder, A.J. Smit, J.J.A.M. van den Dungen, J.M.M. Hooymans, et al., Treatment with intramuscular vascular endothelial growth factor gene compared with placebo for patients with diabetes mellitus and critical limb ischemia: a double-blind randomized trial, Hum. Gene Ther. 17 (2006) 683–691, http://dx.doi.org/10.1089/Hum.2006.17.683.
[13] I. Capila, R.J. Linhardt, Heparin-protein interactions, Angew. Chem. Int. Ed. 41 (2002) 391–412.
[14] A.-K. Olsson, A. Dimberg, J. Kreuger, L. Claesson-Welsh, VEGF receptor signalling — in control of vascular function, Nat. Rev. Mol. Cell Biol. 7 (2006) 359–371, http://dx.doi.org/10.1038/nrm1911.
[15] B.L. Seal, A. Panitch, Physical polymer matrices based on affinity interactions between peptides and polysaccharides, Biomacromolecules 4 (2003) 1572–1582, http://dx.doi.org/10.1021/bm0342032.
[16] D.S.W. Benoit, K.S. Anseth, Heparin functionalized PEG gels that modulate protein adsorption for hMSC adhesion and differentiation, Acta Biomater. 1 (2005) 461–470, http://dx.doi.org/10.1016/j.actbio.2005.03.002.
[17] G. Tae, M. Scatena, P.S. Stayton, A.S. Hoffman, PEG-cross-linked heparin is an affinity hydrogel for sustained release of vascular endothelial growth factor, J. Biomater. Sci. Polym. Ed. 17 (2006) 187–197, http://dx.doi.org/10.1163/156856206774879090.
[18] J.J. Yoon, H.J. Chung, T.G. Park, Photo-crosslinkable and biodegradable pluronic/heparin hydrogels for local and sustained delivery of angiogenic growth factor, J. Biomed. Mater. Res. 83 (2007) 597–605, http://dx.doi.org/10.1002/jbm.a.31271.
[19] N. Yamaguchi, L. Zhang, B.-S. Chae, C.S. Palla, E.M. Furst, K.L. Kiick, Growth factor mediated assembly of cell receptor-responsive hydrogels, J. Am. Chem. Soc. 129 (2007) 3040–3041, http://dx.doi.org/10.1021/ja0680358.
[20] T. Nie, A. Baldwin, N. Yamaguchi, K.L. Kiick, Production of heparin-functionalized hydrogels for the development of responsive and controlled growth factor delivery systems, J. Control. Release 122 (2007) 287–296, http://dx.doi.org/10.1016/j.jconrel.2007.04.019.
[21] A. Nilasaroya, L.A. Poole-Warren, J.M. Whitelock, P. Jo Martens, Structural and functional characterisation of poly(vinyl alcohol) and heparin hydrogels, Biomaterials 29 (2008) 4658–4664, http://dx.doi.org/10.1016/j.biomaterials.2008.08.011.
[22] M. Kim, J.Y. Lee, C.N. Jones, A. Revzin, G. Tae, Heparin-based hydrogel as a matrix for encapsulation and cultivation of primary hepatocytes, Biomaterials 31 (2010) 3596–3603, http://dx.doi.org/10.1016/j.biomaterials.2010.01.068.
[23] Y. Liang, K.L. Kiick, Heparin-functionalized polymeric biomaterials in tissue engineering and drug delivery applications, Acta Biomater. 10 (2014) 1588–1600, http://dx.doi.org/10.1016/j.actbio.2013.07.031.
[24] U. Freudenberg, A. Hermann, P.B. Welzel, K. Stirl, S.C. Schwarz, M. Grimmer, et al., A star-PEG-heparin hydrogel platform to aid cell replacement therapies for neurodegenerative diseases, Biomaterials 30 (2009) 5049–5060, http://dx.doi.org/10.1016/j.biomaterials.2009.06.002.
[25] U. Freudenberg, J.-U. Sommer, K.R. Levental, P.B. Welzel, A. Zieris, K. Chwalek, et al., Using mean field theory to guide biofunctional materials design, Adv. Funct. Mater. 22 (2012) 1391–1398, http://dx.doi.org/10.1002/adfm.201101868.
[26] A. Zieris, S. Prokoph, K.R. Levental, P.B. Welzel, M. Grimmer, U. Freudenberg, et al., FGF-2 and VEGF functionalization of starPEG-heparin hydrogels to modulate biomolecular and physical cues of angiogenesis, Biomaterials 31 (2010) 7985–7994, http://dx.doi.org/10.1016/j.biomaterials.2010.07.021.
[27] A. Zieris, K. Chwalek, S. Prokoph, K.R. Levental, P.B. Welzel, U. Freudenberg, et al., Dual independent delivery of pro-angiogenic growth factors from starPEG-heparin hydrogels, J. Control. Release 156 (2011) 28–36, http://dx.doi.org/10.1016/j.jconrel.2011.06.042.
[28] K. Chwalek, K.R. Levental, M.V. Tsurkan, A. Zieris, U. Freudenberg, C. Werner, Two-tier hydrogel degradation to boost endothelial cell morphogenesis, Biomaterials 32 (2011) 9649–9657, http://dx.doi.org/10.1016/j.biomaterials.2011.08.078.
[29] C.J. Robinson, B. Mulloy, J.T. Gallagher, S.E. Stringer, VEGF165-binding sites within heparan sulfate encompass two highly sulfated domains and can be liberated by K5 lyase, J. Biol. Chem. 281 (2006) 1731–1740, http://dx.doi.org/10.1074/jbc.M510760200.
[30] A. Zieris, R. Dockhorn, A. Röhrich, R. Zimmermann, M. Müller, P.B. Welzel, et al., Biohybrid networks of selectively desulfated glycosaminoglycans for tunable growth factor delivery, Biomacromolecules 15 (2014) 4439–4446, http://dx.doi.org/10.1021/bm5012294.
[31] M. Petitou, J. Lormeau, Interaction of heparin and antithrombin III, the role of O-sulfate groups, Eur. J. Biochem. 176 (1988) 637–640.
[32] P. Sinaÿ, Sugars slide into heparin activity, Nature 398 (1999) 377–378, http://dx.doi.org/10.1038/18783.
[33] L. Ayotte, A.S. Perlin, N.m.r. spectroscopic observations related to the function of sulfate groups in heparin. Calcium binding vs. biological activity, Carbohydr. Res. 145 (1986) 267–277, http://dx.doi.org/10.1016/S0008-6215(00)90434-8.
[34] H. Baumann, H. Scheen, B. Huppertz, R. Keller, Novel regio-and stereoselective O-6-desulfation of the glucosamine moiety of heparin with N-methylpyrrolidinone–water or N, N-dimethylformamide–water mixtures, Carbohydr. Res. 308 (1998) 381–388.
[35] Y. Inoue, K. Nagasawa, Selective N-desulfation of heparin with dimethyl sulfoxide containing water or methanol, Carbohydr. Res. 46 (1976) 87–95, http://dx.doi.org/10.1016/S0008-6215(00)83533-8.
[36] M. Müller, B. Kessler, S. Richter, Preparation of monomodal polyelectrolyte complex nanoparticles of PDADMAC/poly(maleic acid- alt-α-methylstyrene) by consecutive centrifugation, Langmuir 21 (2005) 7044–7051, http://dx.doi.org/10.1021/la050716d.
[37] M.V. Tsurkan, K.R. Levental, U. Freudenberg, C. Werner, Enzymatically degradable heparin-polyethylene glycol gels with controlled mechanical properties, Chem. Commun. 46 (2010) 1141–1143, http://dx.doi.org/10.1039/B921616B.
[38] A. Zieris, S. Prokoph, P.B. Welzel, M. Grimmer, K.R. Levental, W. Panyanuwat, et al., Analytical approaches to uptake and release of hydrogel-associated FGF-2, J. Mater. Sci. Mater. Med. 21 (2009) 915–923, http://dx.doi.org/10.1007/s10856-009-3913-z.
[39] J.R. Weis, B. Sun, G.M. Rodgers, Improved method of human umbilical arterial endothelial cell culture, Thromb. Res. 61 (1991) 171–173.
[40] M.M. Martino, F. Tortelli, M. Mochizuki, S. Traub, D. Ben-David, G.A. Kuhn, et al., Engineering the growth factor microenvironment with fibronectin domains to promote wound and bone tissue healing, Sci. Transl. Med. 3 (2011) 100ra89, http://dx.doi.org/10.1126/scitranslmed.3002614.
[41] R. Takano, Desulfation of sulfated carbohydrates, Trends Glycosci. Glycotechnol. 14 (2002) 343–354.
[42] Y.A. Muller, B. Li, H.W. Christinger, J.A. Wells, B.C. Cunningham, A.M. de Vos, Vascular endothelial growth factor: crystal structure and functional mapping of the kinase domain receptor binding site, Proc. Natl. Acad. Sci. U. S. A. 94 (1997) 7192–7197.
[43] K. Ono, H. Hattori, S. Takeshita, A. Kurita, M. Ishihara, Structural features in heparin that interact with VEGF165 and modulate its biological activity, Glycobiology 9 (1999) 705–711.
[44] X. Huang, C.S. Brazel, On the importance and mechanisms of burst release in matrix-controlled drug delivery systems, J. Control. Release 73 (2001) 121–136.
[45] R. Flaumenhaft, D.B. Rifkin, The extracellular regulation of growth factor action, Mol. Biol. Cell 3 (1992) 1057–1065.
[46] C.A. Reinhart King, Chapter 3. Endothelial cell adhesion and migration, Methods in Enzymology, Elsevier 2008, pp. 45–64, http://dx.doi.org/10.1016/S0076-6879(08)02003-X.
[47] R.B. Vernon, E.H. Sage, A novel, quantitative model for study of endothelial cell migration and sprout formation within three-dimensional collagen matrices, Microvasc. Res. 57 (1999) 118–133, http://dx.doi.org/10.1006/mvre.1998.2122.
[48] D.C. Hoffmann, C. Textoris, F. Oehme, T. Klaassen, A. Goppelt, A. Römer, et al., Pivotal role for alpha1-antichymotrypsin in skin repair, J. Biol. Chem. 286 (2011) 28889–28901, http://dx.doi.org/10.1074/jbc.M111.249979.